Korean J. Chem. Eng., 32(1), 97-103 (2015)
DOI: 10.1007/s11814-014-0198-9

pISSN: 0256-1115
eISSN: 1975-7220

Preparation and investigation of the gas separation properties of polyurethane-TiO_2 nanocomposite membranes

Morteza Sadeghi†, Hajar Taheri Afarani, and Zohreh Tarashi

Department of Chemical Engineering, Isfahan University of Technology, Isfahan 84156-83111, Iran
(*Received 22 October 2013 • accepted 13 July 2014*)

Abstract−The effect of TiO_2 nanoparticles on the gas separation properties of polyurethane has been investigated. Polyurethane was synthesized using hexamethylene diisocyanate (HDI) and 1,4-butanediol (BDO) as hard segment and poly(tetramethylene glycol) (PTMG, 2,000 g/mol) as soft segment. The synthesized polymer was in a 1 : 2 : 1 molar ratio of polyol : diisocyanate : chain extender through bulk two-step polymerization. PU membranes were prepared by thermal phase inversion method. Scanning electron microscopy (SEM), X-ray diffraction and Fourier Transform Infrared (FTIR) analyses characterized the prepared membranes. FTIR and SEM results indicate the good interaction between particles and polymer matrix and also the nanoscale dispersion of TiO_2 particles in polymer matrix. Gas permeation properties of PU-TiO_2 nanocomposite membranes with TiO_2 contents up to 30 wt% were studied for N_2, O_2, CH_4 and CO_2 gases at 10 bar and 25 °C. Results suggest a decrease in permeability of studied gases and increase in gas selectivities as TiO_2 content increases.

Keywords: Gas Separation, Membrane, TiO_2 Nanoparticle, Polyurethane, Nanocomposite

INTRODUCTION

Membrane separation processes are one of the most noteworthy separation techniques because of their remarkable advantages, such as low investment, ease of installation, low maintenance cost, low energy consumption and higher flexibility of product purity. Owing to some super properties, such as low capital cost, ability to move manufacturing easily toward commercial uses that can be processed into modules, steadfastness at high pressures, low energy consumption and facile scalability, polymeric membranes are one of the best candidates in the field of membrane science for use in various gas separation applications (e.g., natural gas processing, landfill gas recovery, separation of olefin/paraffin, air separation, hydrogen recovery, etc.) [1-5]. The basic variables depicting gas separation membranes are the permeability coefficient, P_A, and the selectivity, $\alpha_{AB}(=P_A/P_B)$ [2,4]. In recent decades, different types of polymeric membrane have been investigated for gas separation. However, some of the conventional polymeric membranes exhibit weak gas separation performance as proven by Robeson's tradeoff line between permeability and selectivity, while some of them, such as polyimides, polysulfones, polycarbonates, polyurethanes (PUs) and some other polymers, show acceptable gas separation performance [6].

Recent research shows that PU membranes are good candidates for gas separation membranes because of their high mechanical properties, thermal stability as well as high gas separation performance [7-11]. PUs are a set of polymers with extremely extensive flexibility in their structures and properties, which are comprised of alternating urethane or urea as hard segments and polyol (polyether/polyester) as soft segment. PUs also have excellent mechanical and physical properties with a broad temperature range for a wide variety of uses [12,13]. The hard segments of urethane/urea are formed by extending an extremity diisocyanate with a low molecular weight diol/diamine. The soft segment is made up of polyether/polyester groups with high molecular weight [14]. The properties of PUs are simply fitted, causing restrained changes in polyol chain length, and also changing the proportions and chemical nature of the constituents which form the flexible and rigid segments of the polymer chain [7,10,12-16].

The performance of polymeric membranes in gas separation is the most effective factor in the economy of separation. Therefore, most recent research has been focused on the enhancement of the gas separation properties of polymeric membranes [17,18]; different techniques have been suggested for this purpose. Among them, embedding various inorganic nanoparticles (e.g., zeolites, carbon molecular sieves, alumina, titania (TiO_2), silica and other metal oxides) into a polymer matrix as a filler is mentioned as an efficient technique to improve gas separation properties of different polymeric membranes [19-25]. Polymer/inorganic nanocomposite materials have been optimized to improve the properties of polymers. In this type of membrane, the inorganic phase is dispersed at nanoscale in the polymer phase. Due to the special structural characteristics of polymer/inorganic nanocomposites, they exhibit remarkable properties [26]. A wide variety of nanoparticles has been introduced to modify organic membranes, such as SiO_2, Al_2O_3, Fe_3O_4, ZrO_2 and TiO_2 [23-25] to form so-called nanocomposite membranes. Jadav et al. reported that the incorporation of silica nanoparticles into polyamide could enhance the gas separation performance of

†To whom correspondence should be addressed.
E-mail: m-sadeghi@cc.iut.ac.ir
Copyright by The Korean Institute of Chemical Engineers.

the nanocomposite membranes containing about 1-2 wt% silica [27]. We used the same type of nanoparticles and incorporated them into polyether- and polyester-based PU separately in our previous works [29,30]. The obtained results show that incorporation of silica nanoparticles decreases gas permeability, while increasing the CO_2/N_2 and CO_2/CH_4 gas selectivities in nanocomposite membranes. In another article, we showed that by embedding silica nanoparticles into polybenzimidazole (PBI), the permeability of the condensable gases (i.e., CO_2 & CH_4) was increased, while that of non-condensable gas (i.e., N_2) surprisingly decreased with increasing silica content [4,20]. In addition, we investigated the effect of silica nanoparticles and pressure on the gas separation properties of ethylene vinyl acetate (EVA)-silica nanocomposite membrane [22]. The results show a considerable increase in the permeability of all gases, and improvement in the selectivity of CO_2 over other fixed gases was observed with increasing silica content.

Vijay et al. [30] investigated the effect of different concentrations of $Co_{0.6}Zn_{0.4}Fe_2O_4$ nanoparticle on the gas transport properties of polycarbonate membranes. Their results showed that the permeabilities decrease and gas selectivity increases with increasing concentration of nanoparticles (0.3%-5%) in polymer [30].

Lee et al. [31] used polyphenylene oxide (PPO) as a polymeric precursor for carbon membrane preparation. In their study, the PPO-derived carbon membranes were prepared by carbonization and followed by air oxidation as post-treatment method to modify the membrane pore structures. It was concluded in the oxidation effect on the modification of permeation that the post-oxidation of the carbon membranes in- creases gas permeation and separation properties [31].

Among other nanoparticles, TiO_2 has received much attention because of its good physical and chemical properties, its availability as well as its potential for antifouling abilities [17,32-35]. For instance, Kong et al. [34] reported the PI/TiO_2 nanocomposite membrane for gas separation. They found that embedding TiO_2 nanoparticles into PI showed higher permeability of gases than that of pure PI, and also that by increasing the amount of TiO_2, the selectivity of PI/TiO_2 composite membranes was still kept at a high level, possibly due to the specific interaction between gases and the TiO_2 component in PI/TiO_2 composite membranes. Yave et al. [36] incorporated TiO_2 into poly(4-methyl-2-pentyne) and discovered that the resulting PMP/TiO_2 hybrid nanocomposite membranes displayed an improvement in n-butane permeability and n-butane/methane selectivity. In another work, Ghadimi et al. [37] investigated separation properties of C_3H_8, CH_4, and H_2 through nanocomposite membranes with different nanoparticle contents. Their observations showed that all the nanocomposite membranes have better ideal selectivity in comparison with pure PDMS membrane. Furthermore, their results displayed a reduction in the permeability of gases with increasing silica nanoparticles content [37].

In the present work, we studied the effect of the incorporation of TiO_2 nanoparticles on the gas separation properties of PU membranes. The effect of TiO_2 on the gas permeation properties of PU membranes was not established before and this work is reported here for the first time. The permeabilities of methane, nitrogen, oxygen and carbon dioxide gases were measured at 10 bar pressure and temperature of 25 °C. Finally, the influence of the particles on the separation properties of the gas was explored.

Table 1. Details of particle

Properties	Particle (TiO_2)
Specific surface area (m^2/g)	100-150
Particle size (nm)	10-15
Used formats	Powder

EXPERIMENTAL

1. Materials

Hexamethylene diisocyanate (HDI) and 1,4-butanediol (BDO) were purchased from Merck Company. Poly(tetramethylene glycol) with number-average molecular weight of 2,000 g/mole (PTMG, 2,000 g/mole) was obtained from Arak Petrochemical Complex (Arak, Iran) and dried at 80 °C under vacuum for 48 h to remove residual water. The polymer was synthesized in mole ratio of 1 : 2 : 1 of polyol:diisocyanate:chain extender via bulk two-step polymerization [38]. TiO_2 nanoparticle was purchased from TECNAN Co. (Spain), and the detailed properties of nanoparticles are shown in Table 1. Dimethyl-formamide (DMF) was purchased from Merck. CO_2, N_2 and O_2 gases (purity 99.99) used for gas permeation tests were purchased from Ardestan Gas Co. (Iran) and CH_4 (purity 99.9) was purchased from Technical Gas Service Co. (Iran). The membranes' thicknesses were measured with a micrometer and were about 180 μm.

2. Preparation of PU Membrane

PU membranes were prepared by solution casting and solvent evaporation technique. 10 grams of synthesized polymer were dissolved in 90 g DMF to obtain a 10 wt% solution at 50 °C. The mixture was then stirred for 30 min to form a homogeneous solution. The prepared solution was filtered and casted on a Petri dish. Next the prepared film was placed in a vacuum oven at 60 °C for 24 h to form the membrane. Excess solvent was removed from membranes by placing the prepared films in vacuum oven at 60 °C for 5 additional hours.

3. Preparation of PU-TiO_2 Composite Membrane

PU-TiO_2 nanocomposite membranes were prepared by addition of TiO_2 nanoparticle in different weight fractions (5, 10, 20 and 30 wt%) to the polymer solution (10 wt%). The mixture was then stirred to form a homogeneous solution at 50 °C and atmospheric pressure of 10 bar. Then the dope solution was filtered and casted on a Petri dish. Finally, the prepared film was placed in a vacuum oven at 60 °C for 24 h to remove all of the solvent.

4. Characterization

The presence of TiO_2 nanoparticles in the PU-TiO_2 membranes were investigated by Fourier Transform Infrared spectrometer (FTIR, Bruker-Tensor 27, Germany) in the range of 4,000-600 cm^{-1}. Scanning electron microscope (SEM, KYKY and EM3200) was employed to observe the cross-section morphologies of nanocomposite membranes. The cross sections were prepared by cryogenically fracturing the membranes in liquid nitrogen and then coating with gold before observation. X-ray diffraction patterns (XRD, Philips Co., Poland) were recorded by monitoring the diffraction angle 2θ from 0^o to 50^o using Cu radiation under a voltage of 40 kV and a cur-

rent of 30 mA.

5. Gas Permeability Measurement

Transportation of gases through a nonporous dense polymer membrane is generally depicted by solution-diffusion mechanism. According to this mechanism, the penetrants dissolve into the polymer matrix at upstream surface (high pressure), then diffuse across the polymer film and finally desorb from the downstream face [39]. The permeability of nitrogen, methane, oxygen and carbon dioxide were determined using the constant pressure/variable volume method at 10 bar and 25 °C [40]. The gas permeability of membranes was determined using the following equation:

$$P = \frac{ql}{A(P_1 - P_2)} \quad (1)$$

where P is permeability expressed in barrer (1 barrer=10^{-10} cm^3 (STP) cm/cm^2 s cm Hg), q is the flow rate of the permeate gas passing through the membrane (cm^3 (STP)/s), l is the membrane thickness (cm), p_1 and p_2 are the absolute pressures of feed side and permeate side, respectively (cm Hg), and A is the effective membrane area (cm^2). The ideal selectivity (or permselectivity), $\alpha_{A/B}$, of membranes was calculated from pure gas permeation experiments:

$$\alpha_{A/B} = P_A/P_B \quad (2)$$

Following each test, the remaining gases from the previous experiment were removed from the permeation system by purging the stream lines with fresh gas, which was considered for test.

RESULTS AND DISCUSSION

1. FTIR Analysis

Structural characteristics of pure TiO_2 nanoparticle, PU and PU-TiO_2 hybrid membranes were carried out using FTIR analysis. The FTIR spectra of prepared membranes and nanoparticle were shown in Fig. 1. As can be seen, the strong peak at 577 cm^{-1}, which belongs to TiO_2, is observed in TiO_2 nanoparticle and all nanocomposite membranes, confirming the presence of nanoparticles in hybrid membranes. The peaks related to the N-H bonds of urethane groups in the membranes are also can be observed in the range of 3,300

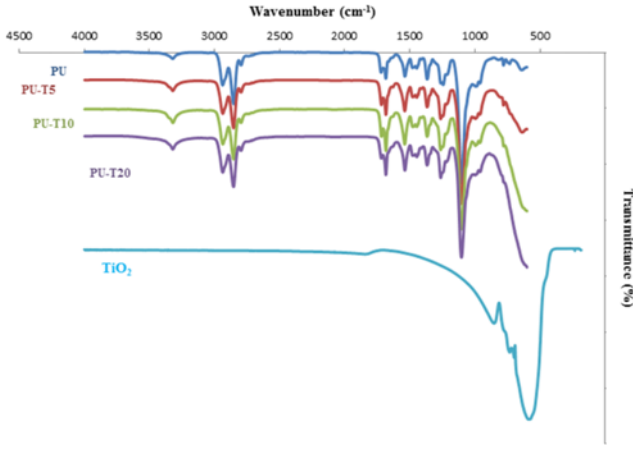

Fig. 1. ATR-FTIR spectra of PU, TiO_2 nanoparticle and PU-TiO_2 hybrid membranes.

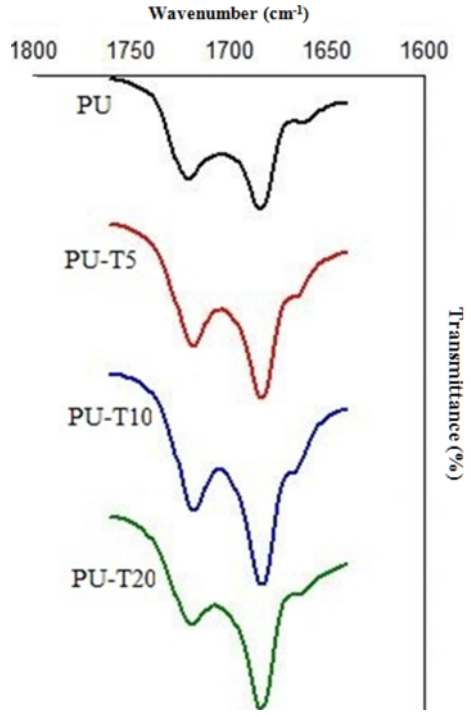

Fig. 2. ATR-FTIR spectra in the range of 1,640-1,760 cm^{-1} for prepared membranes.

cm^{-1}. To explore the effects of TiO_2 nanoparticles on the phase separation of hard and soft segments of prepared membranes, one can evaluate the peaks related to the carbonyl groups. Fig. 2 shows the absorption of urethane carbonyl groups in pure polymer and hybrid membranes. The peak appeared in a lower wave number (around 1,683 cm^{-1}), referring to the bonded, and one appeared in a higher wave length (around 1,720 cm^{-1}), referring to the free carbonyls [38,40-42]. As seen in Fig. 2, the intensity of the peak related to bonded carbonyl in comparison to free carbonyl increases with an increasing amount of TiO_2 in polymer. The Hydrogen Bond Index (HBI), the proportion of +intensity of the bonded C=O to the free C=O, of prepared membranes is an acceptable index to illustrate the phase separation in PU changes as follows:

1.26 (PU)<1.38 (PU-T5)<1.55 (PU-T10)<1.75 (PU-T20)

As reported previously, the phase separation increases in PU with enhancement of HBI. This observation indicates more hydrogen bonding among urethane carbonyl groups and urethane N-H groups in hard segments. Given the obtained results, it would be concluded that by interaction of most of the population of TiO_2 nanoparticles to ether groups in soft segments, the carbonyl groups in hard segments would interact more with N-H urethane groups in hard segments and therefore, phase separation may increase by boosting the amount of nanoparticles. Consequently, it can arise from FTIR study that TiO_2 nanoparticles interact more with ether groups of polyol in soft segments or urethane N-H groups in the boundary of PU. Consequently, it can be concluded that most of the TiO_2 nanoparticles are dispersed in soft segments in PU [22,24,29].

2. Morphology of PU-TiO_2 Nanocomposite Membranes

The presence and distribution of TiO_2 nanoparticles in the PU

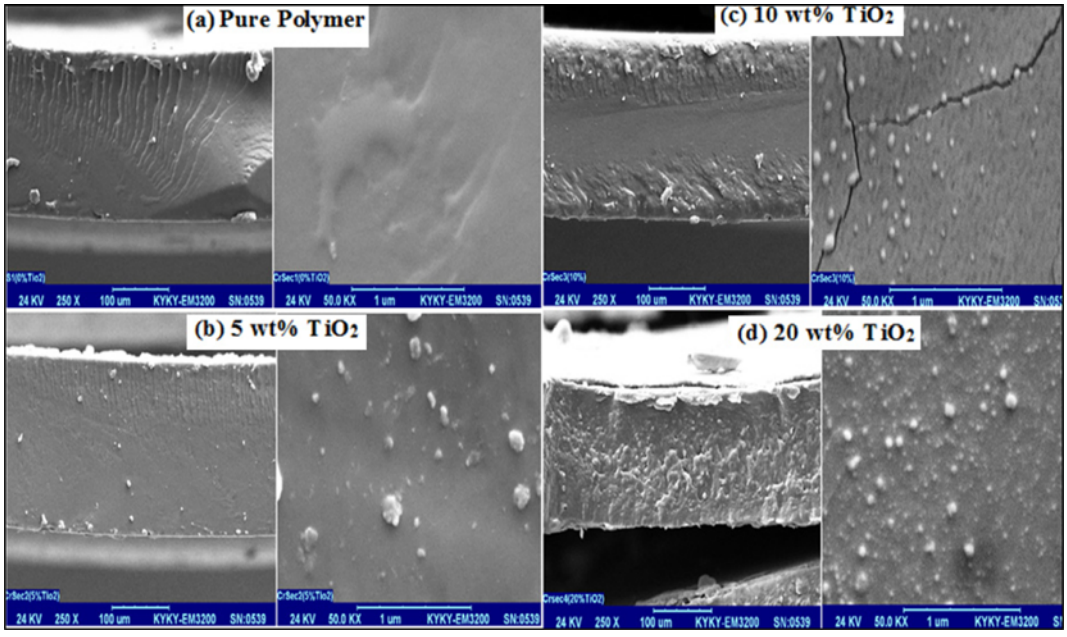

Fig. 3. SEM images of the cross section of polyurethane and hybrid PU containing TiO_2 nanoparticles in different magnification (250× and 50,000×). (a) Pure PU (b) PU-5 wt% TiO_2 (c) PU-10 wt% TiO_2 (d) PU-20 wt% TiO_2.

membranes has been studied by SEM. Figs. 3(a), 3(b), 3(c) and 3(d) show the SEM of the prepared PU-TiO_2 hybrid membranes. As can be seen, the membranes are quite dense and the presence and nanometric distribution of TiO_2 particles in prepared membranes are evident. The SEM micrographs show well the distribution of the particles in polymer matrix. Behind the nanoscale dispersion of particles, some agglomerate particles in the range of 150-200 nm are also evident in the matrix.

3. XRD Analysis

The structural changes induced by the presence of TiO_2 domains were characterized by X-ray diffraction. XRD patterns of PU-TiO_2 hybrids containing 5, 10 and 20 wt% TiO_2 were compared with that of pure PU and TiO_2 nanoparticles, as shown in Fig. 4. In general, when a polymer contains a large crystalline region, the peak observed in the XRD patterns of the polymer is usually sharp and intensity is strong, whereas that of amorphous polymer is rather broad [20,38,41,43]. As shown in Fig. 4, there is a broad peak around 2θ=20.4° in pure PU. This broad peak confirms the presence of amorphous structure in pure PU membrane that exists in the 5, 10 and 20 wt% TiO_2 membranes. The pattern of TiO_2 crystal nanoparticles has three significant crystalline characteristic peaks at 2θ= 25.445° (101), 37.900° (004) and 48.170° (200), which agree with the literature [44]. Additionally, these mentioned crystalline peaks of TiO_2 nanoparticle appeared in the 5, 10 and 20 wt% PU-TiO_2 nanocomposite membranes. The presence of crystalline peaks of TiO_2 nanoparticles indicates the TiO_2 particles that existed in the nanocomposite membranes were not in amorphous form. The crystalline peaks observed in the XRD patterns at the 5, 10 and 20 wt% of PU-TiO_2 nanocomposite membranes became sharper and the intensities stronger with the effect of the TiO_2 nanoparticle. The increase in crystallinity suggests that the interface adhesion is strong between inorganic additives and organic polymer structure due to the structural modification [45-47].

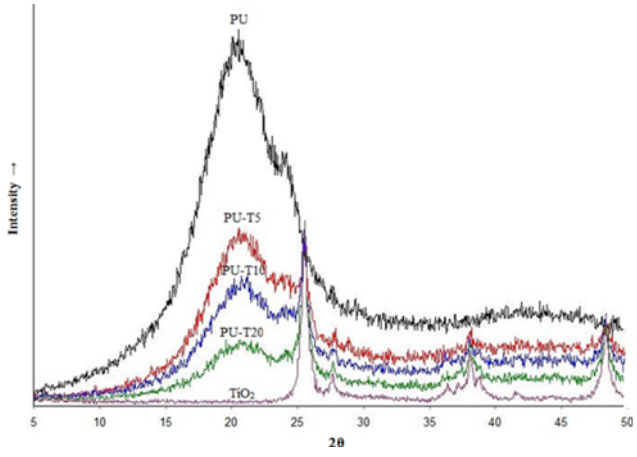

Fig. 4. XRD patterns obtained for PU, TiO_2 nanoparticle and PU-TiO_2 hybrid membranes.

4. Gas Permeation

The permeation of CO_2, N_2, CH_4 and O_2 gases has been measured at 10 bar and 25 °C. The permeability of gases through PU and PU-TiO_2 hybrid membranes versus the amount of TiO_2 nanoparticles in polymers is shown in Fig. 5. As shown, for all membranes, the permeabilities decrease in the order of P (CO_2)>>P (CH_4) >P (O_2)>P (N_2). As shown in this figure, the permeability of CO_2 is significantly higher than those of other gases in all pure and composite membranes. The high permeation rate of CO_2 in comparison with other studied gases is due to its low kinetic diameter, high condensability and the greater interaction of this polar gas with polar groups in polymer [29,40]. As shown in Table 2, the kinetic diameter of methane is greater than nitrogen and oxygen mole-

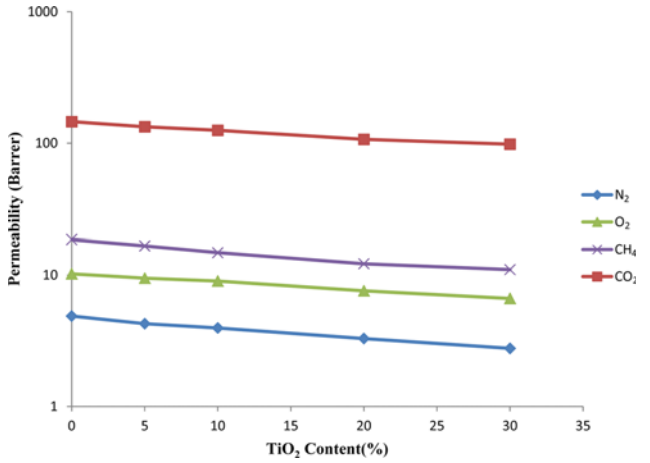

Fig. 5. Effect of TiO_2 content in polyurethane-TiO_2 membranes on permeability of studied gases.

Table 2. Physical properties of penetrants

Gas	Kinetic diameter (°A)	Condensability (K)
CO_2	3.3	195
O_2	3.46	107
N_2	3.64	71
CH_4	3.8	149

cules, but the permeability reported in Fig. 5 indicates more permeation of methane in comparison with oxygen and nitrogen [48]. This discrepancy can be explained by the known solution-diffusion mechanism [2, 38]. Due to this mechanism the higher condensation property of methane improves the solution of methane in polymer and leads to greater permeability of this gas in the PU and PU-TiO_2 hybrid membranes compared to nitrogen and oxygen. As is known, the solution mechanism is dominant in the permeation of gases through rubbery polymers. Therefore, the obtained results would show the high rubbery properties of pure and composite membranes. Fig. 5 also shows the gas permeability of membranes reduced by increasing the amount of TiO_2 nanoparticles in polymer. It is recognized that the permeation of gases occurs more in the soft segments in PU membranes, and hard segments are impermeable barrier regions in PUs. In addition, the investigation by FTIR of prepared membranes showed that, by increasing the content of TiO_2 in polymer, most of the TiO_2 nanoparticles may be dispersed in soft segments. The results obtained in the gas permeation test confirm the FTIR study. The reduction in the gas permeabilities could be attributed to two factors. The first might be the increased tortuosity of the diffusion path, in which the presence of additional substances such as non-permeable TiO_2 particles reduces the free volume of soft segments, changes the passage areas of gas molecules and makes diffusion path a tortuous one. The second is the decrease in free volume, which reduces the sorption and diffusion of penetrants in the polymer matrix [8,37,49]. Therefore, the permeation of gases decreases by increasing the amount of TiO_2 nanoparticles in polymer. Comparison of gas permeability in PU and PU-TiO_2 composites (as shown in Fig. 5) demonstrates that the gas permeabilities of carbon dioxide, methane, oxygen and nitrogen in the pure polymer decrease from 145, 18.50, 10.20 and 4.90 barrer to the amount of 98, 11, 6.6 and 2.8 barrer in the PU-TiO_2 (30 wt%) composite membrane, respectively. Calculated reduction values of gas permeability of prepared nanocomposite membranes with respect to pure PU are in the following order:

CO_2 (32.62%)<O_2 (35.10%)<CH_4 (40.65%)<N_2 (43.18%).

By reducing the amount of free volume of the polymer, the gas molecules of larger size are more restricted from crossing the polymer thickness than smaller ones, and thus their permeabilities will decrease more [29,40]. Therefore, the higher reduction of N_2 permeability in comparison with CO_2 and O_2 is due to its large molecular size, and this makes sense because of the presence of TiO_2 nanoparticles. Due to their non-organic nature, TiO_2 nanoparticles would create some suitable sites in the interface of organic polymer and non-organic particles which are suitable for dissolution of condensable gases [29]. Therefore, by increasing the content of TiO_2 in polymer, dissolution of condensable methane gas will increase, and despite its molecular size being larger than N_2, its permeability decreases more slowly. Regarding CO_2, its lower reduction of permeability with increasing TiO_2 compared to other gases results from both its small molecular size and its greater solubility in the membrane, because of the increased polar groups in the polymer with increasing TiO_2 content. Good interaction between polar CO_2 and polar groups in TiO_2 increases the dissolution of CO_2 in the polymer.

Fig. 6 shows the CO_2/N_2, CO_2/CH_4 and O_2/N_2 selectivities of PU and PU-TiO_2 hybrid membranes. As shown in this figure, by increasing the TiO_2 content in nanocomposites, all selectivities increased. Fig. 6 shows that CO_2/N_2, CO_2/CH_4 and O_2/N_2 selectivities increase from 29.90, 7.8 and 2.10 for pure PU to 35.40, 8.9 and 2.40 for PU-TiO_2 (30 wt%). The order of increment in gas selectivity of the hybrid membranes by addition of TiO_2 nanoparticles is as follow:

CO_2/N_2 (18.6%)>O_2/N_2 (13.9%)>CO_2/CH_4 (13.65%).

The enhancement of gas selectivity with the addition of TiO_2 nanoparticles is due to improvement in the molecular sieve property of the hybrid membranes. As mentioned before, most of the particles may disperse in soft segments. Therefore, the presence of the par-

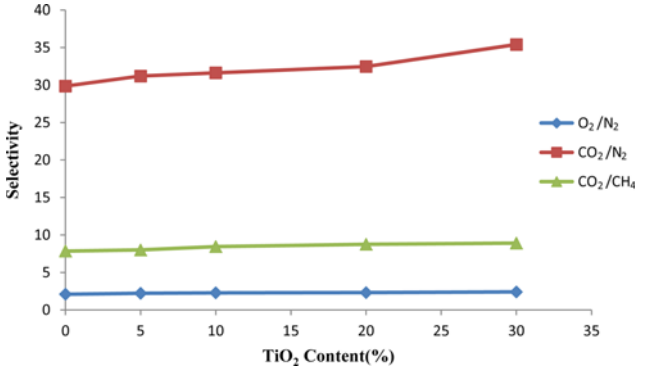

Fig. 6. Permselectivity of CO_2/N_2, CO_2/CH_4 and O_2/N_2 gases in PU and PU-TiO_2 nanocomposite membranes versus weight fraction of TiO_2 in polymer.

ticles should affect the mobility of the polymer chains in soft segments and also may reduce the free spaces trapped in the soft segments. These two events would increase the molecular sieving property of the hybrid membrane and lead to improvement of the hybrid membrane's ability to select the small molecules rather than larger molecules. The higher improvement in CO_2/N_2 selectivity is due to more condensable property and also more interaction of CO_2 molecule with polymer chains in comparison with nitrogen. It means that solubility selectivity also has an effective role on the enhancement of the selectivity of pair gases. Therefore, the enhancements in CO_2/N_2 selectivities are greater than those of O_2/N_2 and CO_2/CH_4 selectivities. As mentioned before, PI/TiO_2 nanocomposite membranes show higher permeability and gas selectivity in comparison to pure PI [34]. The different effect of TiO_2 on gas permeation of PI and PU membranes can be attributed to the mobility of the chains. In PI membrane, because of the low mobility of its chains, the nanoparticles act as spheres between the chains and increase the spaces for permeation of gases, while in PU they may occupy the free volumes and decrease permeability.

CONCLUSIONS

PU-titania nanocomposite membranes were prepared by the solution blending and casting method. In this regard, PU was synthesized using poly(tetramethylene glycol), hexamethylene diisocyanate and 1,4-butanediol. The gas separation properties of the prepared membranes were studied using N_2, O_2, CH_4 and CO_2 gases under atmospheric temperature and pressure. The structure of membranes was characterized using FTIR, SEM and XRD methods.

The obtained results from FTIR and SEM show appropriate distribution of titania nanoparticles in the prepared samples. The gained results from XRD also show the crystalline form of membranes. The gas permeation properties of nanocomposite membranes also showed a decrease in gas permeability of membranes and an increase in CO_2/N_2, O_2/N_2 and CO_2/CH_4 selectivity with increasing titania content.

REFERENCES

1. J. W. Phair and S. P. S. Badwal, *Sci. Tech. Adv. Mater.*, **7**, 792 (2006).
2. Y. Yampolskii, I. Pinnau and B. Freeman, *Materials science of membranes for gas and vapor separatio*n, John Wiley & Sons Publications, England (2006).
3. A. Javaid, *Chem. Eng. J.*, **112**, 219 (2005).
4. M. Pakizeh, A. N. Moghadam, M. R. Omidkhah and M. Namvar-Mahboub, *Korean J. Chem. Eng.*, **30**, 751 (2013).
5. B. D. Freeman, *Macromolecules*, **32**, 375 (1999).
6. L. M. Robeson, *J. Membr. Sci.*, **320**, 390 (2008).
7. X. Jiang, J. Ding and A. Kumar, *J. Membr. Sci.*, **323**, 371 (2008).
8. Y. Chen, R. Wang, J. Zhou, H. Fan and B. Shi, *Polymer*, **52**, 1856 (2011).
9. A. Woliñska-Grabczyk and A. Jankowski, *Sep. Purif. Technol.*, **57**, 413 (2007).
10. J. M. Yang, W. C. Lai and H. T. Lin, *J. Membr. Sci.*, **183**, 37 (2001).
11. H. Li, B. D Freeman and O. Max Ekiner, *J. Membr. Sci.*, **369**, 49 (2011).
12. L. S. Teo, C. Y. Chen and J. F. Kuo, *J. Membr. Sci.*, **141**, 91 (1998).
13. L. S. Teo, J. F. Kuo and C. Y. Chen, *Polymer*, **39**, 3355 (1998).
14. L. Ning, W. D. Ning and Y. S. Kang, *Macromolecules*, **30**, 4405 (1997).
15. M. Ulbricht, *Polymer*, **47**, 2217 (2006).
16. J. M. Yang, H. T. Lin and S. J. Yang, *J. Membr. Sci.*, **258**, 97 (2005).
17. H. Cong, M. Radosz, B. F. Towler and Y. Shen, *Sep. Purif. Technol.*, **55**, 281 (2007).
18. Y. Yampolskii, *Macromolecules*, **45**, 3298 (2012).
19. T. H. Weng, H. H. Tseng and M. Y. Wey, *Int. J. Hydrog. Energy*, **34**, 8707 (2009).
20. M. Sadeghi, M. A. Semsarzadeh and H. Moadel, *J. Membr. Sci.*, **331**, 21 (2009).
21. A. Car, C. Stropnik, W. Yave and K. V. Peinemann, *Sep. Purif. Technol.*, **62**, 110 (2008).
22. M. Sadeghi, G. Khanbabaei, A. H. Saeedi Dehaghani, M. Sadeghi, M. A. Aravand, M. Akbarzade and S. Khatti, *J. Membr. Sci.*, **322**, 423 (2008).
23. L. Yan, S. Y. Li, C. B. Xiang and S. Xianda, *J. Membr. Sci.*, **276**, 162 (2006).
24. L. Y. Yu, Z. L. Xu, H. M. Shen and H. Yang, *J. Membr. Sci.*, **337**, 257 (2009).
25. A. Bottino, G. Capannelli and A. Comite, *Desalination*, **146**, 35 (2002).
26. B. M. Novak, *J. Adv. Mater.*, **5**, 422 (1993).
27. G. L. Jadav and P. S. Singh, *J. Membr. Sci.*, **328**, 257 (2009).
28. M. Sadeghi, M. M. Talakesh, B. Ghalei and M. Shafiei, *J. Membr. Sci.*, **427**, 21 (2013).
29. M. Sadeghi, M. A. Semsarzadeh, M. Barikani and M. Pourafshari Chenar, *J. Membr. Sci.*, **376**, 188 (2011).
30. Y. K. Vijay, V. Kulshrestha, K. Awasthi, N. K. Acharya, A. Jain, M. Singh and D. K. Avasthi, *J. Polym. Res.*, **13**, 357 (2006).
31. H. Lee, H. Suda, K. Haraya and D. Kim, *Korean J. Chem. Eng.*, **23**, 435 (2006).
32. X. Cao, J. Ma, X. Shi and Z. Ren, *Appl. Surf. Sci.*, **253**, 2003 (2006).
33. U. Diebold, *Surf. Sci. Rep.*, **48**, 53 (2003).
34. Y. Kong, H. Du, J. Yang, D. Shi, Y. Wang, Y. Zhang and W. Xin, *Desalination*, **146**, 49 (2002).
35. Z. L. Xu, L. Y. Yu and L. F. Han, *Front. Chem. Eng. China*, **3**, 318 (2009).
36. W. Yave, S. Shishatskiy, V. Abetz, S. Matson, E. Litvinova, V. Khotimskiy and K. V. Peinemann, *Macromol. Chem. Phys.*, **208**, 2412 (2007).
37. A. Ghadimi, S. Norouzbahari, M. Sadrzadeh and T. Mohammadi, *Polym. Adv. Technol.*, **23**, 1101 (2012).
38. M. Sadeghi, M. A. Semsarzadeh, M. Barikani and B. Ghalei, *J. Membr. Sci.*, **354**, 40 (2010).
39. J. G. Wijmans and R. W. Baker, *J. Membr. Sci.*, **107**, 1 (1995).
40. M. A. Semsarzadeh, M. Sadeghi, M. Barikani and H. Moadel, *Iran. Polym. J.*, **16**, 819 (2007).
41. M. Sadeghi, M. A. Semsarzadeh, M. Barikani and B. Ghalei, *J. Membr. Sci.*, **385-386**, 76 (2011).
42. M. A. Semsarzadeh, M. Sadeghi and M. Barikani, *Iran. Polym. J.*, **17**, 431 (2008).
43. J. H. Kim and Y. M. Lee, *J. Membr. Sci.*, **193**, 209 (2001).
44. T. Zhu, Y. Lin, Y. Luo, X. Hu, W. Lin, P. Yu and C. Huang, *Carbohydr. Polym.*, **87**, 901 (2012).

45. D. Yang, J. Li, Z. Jiang, L. Lu and X. Chen, *Chem. Eng. Sci.*, **64**, 3130 (2009).
46. I. Eroglu, Y. Devrim, S. Erkan, N. Bac, D. Stolten, T. Grube (Eds.), *Proceedings of the 18th World Hydrogen Energy Conference (WHEC)* (2010).
47. R. Vijayalakshmi and V. Rajendran, *Arch. Appl. Sci. Res.*, **4**, 1183 (2012).
48. S. A. Mousavi, M. Sadeghi, M. Y. Motamed-Hashemi, M. Pourafshari Chenar, R. Roosta-Azad and M. Sadeghi, *Sep. Purif. Technol.*, **62**, 642 (2008).
49. T. W. Pechar, Faculty of the Virginia Polytechnic and State University (2004).